Contents lists available at ScienceDirect

Materials Science in Semiconductor Processing

Distribution of barrier heights in metal/n-InAlAs Schottky diodes from current–voltage–temperature measurements

CrossMark

N. Hamdaoui [a,*], R. Ajjel [a], B. Salem [b], M. Gendry [c]

[a] Laboratoire des Energies et des Matériaux (LABEM), LR11ES34, Ecole Supérieur des Sciences et de la Technologie Hammam Sousse (ESSTHS), Université de Sousse, Sousse 4011, Tunisia
[b] Laboratoire des Technologies de la Microélectronique (LTM), UMR5129, CNRS-UJF, CEA-Grenoble, 17 Rue des Martyrs, F-38054 Grenoble, France
[c] Université de Lyon, Institut des Nanotechnologies de Lyon (INL)-UMR5270-CNRS, UMR-5270 CNRS, Ecole cenrale de Lyon, 69134 Ecully, France

ARTICLE INFO

ABSTRACT

The current–voltage characteristics of metal/n-InAlAs Schottky diodes were determined in the temperature range 90–300 K. Analysis of the measured characteristics allows the determination of the electrical parameters, the saturation current I_0, the ideality factor n and the serial resistance R_s. The results show an increase of the Schottky barrier height φ_{b0} and a decrease of the ideality factor n both with the increase of the temperature. The characteristics have been interpreted based on the thermionic emission (TE) mechanism with Gaussian distribution of the barrier heights of $\overline{\varphi}_{b0}$ is 0.96 eV and standard deviation σ_{so} is equal to 0.128 V. In addition, the $\ln(I_0/T^2)$ vs. $1/T$ plot yields the effective Richardson constant of 4.65×10^{-3} A cm^{-2} K^{-2} for the metal/InAlAs diode which is lower than the known value of 10.1 A cm^{-2} K^{-2} for InAlAs. The modified Richardson plot shows a straight line relationship between $\ln(I_s/T^2)-(q^2\sigma_{so}^2/2k^2T^2)$ vs. $1000/T$, and gives a value of $A^*=9.2$ A cm^{-2} K^{-2}.

© 2014 Elsevier Ltd. All rights reserved.

1. Introduction

The metal/semiconductor (MS) contact is a simple and important technology in semiconductor devices. A full understanding of the nature of their electrical characteristics is of great technological importance in the electronics industry [1–3]. These types of devices have gained increasing importance due to a wide variety of optoelectronic and high frequency applications. The performance of the Schottky diodes is dominated by the properties of the barrier of the contact interface [4–6]. In order to understand the conduction mechanism of the Schottky barrier diodes (SBDs), many attempts have been made.

Generally, the SBD parameters are determined over a wide range of temperatures in order to understand the nature of the barrier and the conduction mechanism. The analysis of the current–voltage (I–V) characteristics of Schottky barriers on the basis of thermionic emission diffusion (TED) theory reveals an abnormal decrease of the barrier height (BH) and increase of the ideality factor with decreasing temperature [7]. Explanation of the possible origin of such anomalies has been proposed by taking into account the interface state density distribution [7],quantum-mechanical tunneling [8,9], image-force lowering and most recently the lateral distribution of BH inhomogeneities [10,11]. In addition, a Gaussian distribution of the BH over the contact area has been assumed to describe the inhomogeneities as another way too [12]. The barrier height is a fundamental parameter for the rectifying contacts. It is clearly important to understand the true physical origin of

* Corresponding author.
   E-mail address: hamdaoui_nejeh@yahoo.fr (N. Hamdaoui).

such non-ideal behavior so that it can be controlled in future device applications. That is, the determination of the homogeneous barrier height of the device by means of the BH inhomogeneity model is essential for future efforts to reduce and eliminate it [13–15]. The BH inhomogeneity leads to large ideality factors, therefore, it is not surprising that the ideality factor may be improved by improving the uniformity of interface structure.

The ternary alloy III–V compound semiconductor In_xAl_{1-x} As has a direct band gap for $x > 0.32$, its lattice constant matches that of InP for $x=0.523$, where its fundamental band gap, at room temperature, $E_g=1.46$ eV. Its conduction and valence band edge discontinuities with respect to an InP heterojunction are 0.52 and 0.40 eV, respectively. It is also lattice matched to the smaller band gap, $E_g=0.75$ eV, high electron mobility, ternary alloy, $In_{0.53}Ga_{0.47}As$. These properties make it a potentially useful material for a variety of discrete and integrated circuit high-frequency, optoelectronic and microwave device applications which include quantum well and quantum dot structures [16–19].

In this work, a detailed analysis of the I–V characteristics of metal–InAlAs Schottky contacts has been carried out in the temperature range 90–300 K to clarify the origin of the anomalous behavior of temperature dependence of the Schottky diode parameters such as the SBH, ideality factor, Richardson's constant and series resistance (RS). These results have been explained on the basis of a thermionic emission (TE) mechanism with lateral inhomogeneities at the metal–InAlAs interface.

2. Experimental details

The sample under investigation was grown on n+-type doped InP substrate by solid-source molecular beam epitaxy (MBE). The high doping affects the band gap shrinkage and by a band tail extending into the gap. In the heterojunction-based devices, the band gap shifts due to heavy doping result in valence and conduction band discontinuity of the heterojunction interface [20]. After thermal deposition at 565 °C of InP ($n=10^{16}$ cm^{-3}), the $In_{0.52}Al_{0.48}As$ epilayer, lattice matched with InP (0 0 1) was grown. The epilayer was Si-doped at 3×10^{16} cm^{-3} (n-type material). Its growth temperature was fixed at 525 °C, the growth rate was 1 μm/h and the V/III beam equivalent pressure (BEP) ratio was 20. Back side ohmic contact was formed by using e-beam evaporation of Ge/Ni/Au alloy on the n+ substrate followed by rapid thermal annealing process at $T=300$ °C. The Schottky metallization material consisting of 20 nm Ti/Pd/Au evaporated onto InAlAs through a contact mask.

The fabrication of Ohmic contacts frequently includes a high temperature step so that the deposited metals can either alloy with the semiconductor or the high-temperature anneal reduces the unintentional barrier at the interface (in an effort to further improve the contact resistivity). A metal–semiconductor junction results in an Ohmic contact if the Schottky barrier height is zero or negative (back side). In such case, the carriers are free to flow in or out of the semiconductor so that there is a minimal resistance across the contact. For an n-type

semiconductor, this means that the workfunction of the metal must be close to or smaller than the electron affinity of the semiconductor.

Current–voltage (I–V) measurements of the devices were first measured using the Keithley model 4200 semiconductor characterization system in the temperature range 90–300 K by steps of 30 K in the dark.

3. Results and discussion

3.1. Forward-bias I–V characteristics

The current–voltage (I–V) characteristics were widely used to study the performance of Schottky contacts since they present many important device parameters. The current through a Schottky barrier diode is due to thermionic emission current and is given by the relations [21,22]:

$$I = I_0 \left[\exp\left(\frac{qV}{nkT}\right) - 1 \right] \qquad (1)$$

$$I_0 = AA^*T^2 \exp\left(-\frac{q\varphi_{B0}}{kT}\right) \qquad (2)$$

where n is the ideality factor, I_0 is the saturation current, q is the electronic charge, A is the Schottky contact area, T is the absolute temperature in Kelvin, and φ_{B0} is the Schottky effective barrier height. A^* is the effective Richardson constant, where

$$A^* = \frac{4\pi m^* q k^2}{h^3} = \frac{m^*}{m_0} 120A \text{ cm}^{-2} \text{ K}^{-2} \qquad (3)$$

For InAs and AlAs, the electron effective masses are $0.023m_0$ and $0.15m_0$, as given by Palic et al. [23] and Stukel et al. [24] respectively. Using these values, Vegard's law yields $m^*=0.084m_0$ for InAlAs, corresponding to $A^*=10.1$ A cm^{-2} K^{-2} [25].

The ideality factor n can be determined from the slope of linear region of the forward bias ln(I)–V characteristic as

$$n = \frac{q}{kT} \frac{dV}{d\ln(I)} \qquad (4)$$

For an ideal diode $n=1$, but it is usually greater than unity for real diode structures. Actually, the ideality factor is a parameter indicating the Schottky barrier uniformity. In a more uniform interface structure, it has a value closer to the ideal case. On the other hand, the effective barrier height φ_{B0} can be obtained from Eq. (2) as

$$\varphi_{B0} = \frac{kT}{q} \ln\left(\frac{T^2 AA^*}{I_0}\right) \qquad (5)$$

Fig. 1 shows the semilog I–V characteristics of the metal/n-InAlAs Schottky diodes for a temperature range between 90 and 300 K. For V in the 0.2–0.6 V range, the I–V curves become closer to each other, which indicates some contribution of tunnel current. Thermionic emission also began to dominate at higher temperature with medium bias. The downward curvature (non-linear region) in the I–V characteristic at high forward bias values is attributed to a continuum of surface states, which are in equilibrium with the semiconductor, apart from the effect of series resistance [1]. As shown in Fig. 1 the Schottky contacts
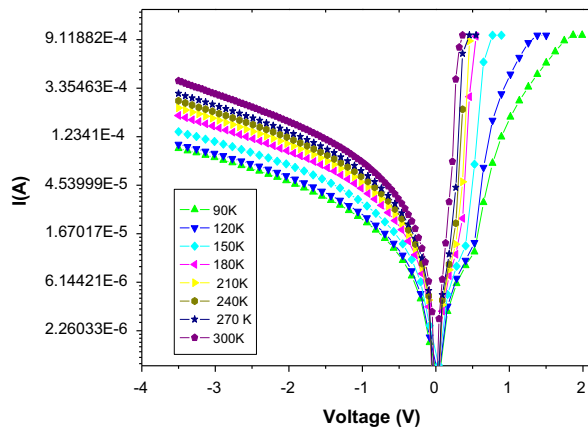
Fig. 1. Forward bias *I–V* characteristics for metal/n-InAlAs Schottky diode in the temperature range of 90–300 K.

Fig. 2. Temperature dependence of the zero-bias barrier height and ideality factor for the metal/n-InAlAs Schottky barrier diode.

Fig. 3. Zero-bias barrier height vs. ideality factor of metal/n-InAlAs Schottky diode at different temperatures.

exhibit quite good diode behavior for all temperature values. The values of the ideality factor (*n*) and barrier height (φ_{B0}) were calculated from the forward *I–V* characteristics presented in Fig. 1 using Eqs. (4) and (5), respectively. The variations of n and φ_{B0} with temperature are plotted in Fig. 2. The value of (*n*)and (φ_{B0}) for metal/n-InAlAs Schottky diode measured over a wide range of temperature (90–300 K) have ranged from 1.81 at 90 K to 1.02 at 300 K, and from 0.18 eV at 90K to 0.85 eV at 300 K, respectively. As expected, while φ_{B0} increase with an increase in temperature, *n* decreases. Since current transport across the metal/semiconductor interface is a temperature activated process, electrons at low temperatures are able to surmount the lower barriers and therefore current transport will be dominated by current flowing through the patches of lower the Schottky barrier height [26]. When temperature increases, more and more electrons have sufficient energy to surmount the higher barrier. Consequently, the dominant barrier will increase with temperature and bias voltage.

The barrier height value of 0.85 eV at 300 K that we have obtained for the metal/n-InAlAs device due to InAlAs layer is remarkably higher than that achieved with conventional MS contact such as metal/n-InP diode, whose barrier height was 0.53 eV [27]. The InAlAs layer forms a physical barrier between the metal and the n-InP wafer. This layer can produce substantial shift in the work function of the metal and in the electron affinity of the semiconductor and in turn, the InAlAs gives an excess barrier of 0.32 eV, i.e., the InAlAs layer increases the barrier height of metal/n-InP. Many attempts to increase or modify the barrier height of Schottky barrier diodes have performed by forming an interfacial layer between the metal and the semiconductor [28,29].

The high values of the ideality factor show that there is a deviation from thermionic emission theory for current mechanism. The increase in ideality factor with decreasing temperature is known as T_0 effect [30]. Such a phenomenon may be due to the interface state density at the metal/semiconductor interface, image force lowering and tunneling of the carrier through the barrier [30]. (*n*) was found to be inversely proportional to temperature as
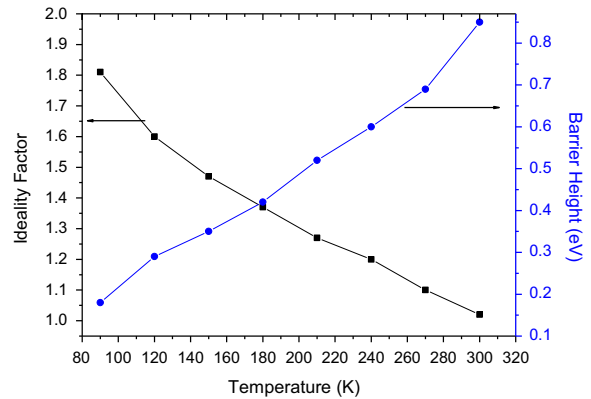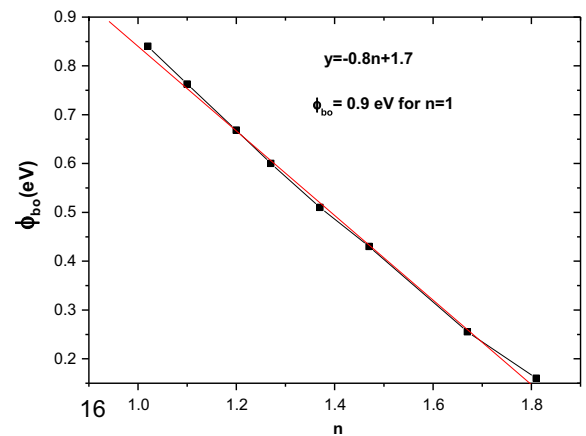
$$n(T) = n_0 + \frac{T_0}{T} \tag{6}$$

where n_0 and T_0 are constants which were found to be 0.51 and 72.3 K, respectively.

There is linear correlation between experimental value of (φ_{B0}) and (*n*) as calculated experimentally. This linear dependence of (φ_{B0}) and (*n*) has theoretically and experimentally reported by Tung et al. [4]. Fig. 3 shows a graph between φ_{B0} vs. *n* for various temperatures. There is a linear relationship between the (φ_{B0}) and (*n*), which has been explained by lateral inhomogeneities [31] of the BHs in the metal/n-InAlAs diode. The extrapolation of φ_{B0} vs. *n* plot to *n*=1 has given a homogeneous φ_{B0} of approximately 0.9 eV. The significant decrease of the zero-bias (φ_{B0}) and increase of (*n*) especially at low temperature are possible caused by the (φ_{B0}) inhomogeneities at metal/semiconductor contact [32].

There are several methods to obtain the R_s value. The presence of R_s in the structure is responsible for the deviation of *I–V* characteristics from linearity. Here, R_s has been calculated by using a method developed by

Cheung and Cheung [33]. According to Cheung and Cheung, the forward-bias I–V relation with R_s value be expressed as

$$\frac{dV}{d(\ln I)} = IR_s + \frac{nkT}{q} \tag{7}$$

A plot of $(dV/d(\ln I))$ vs. I will be linear and its slope gives R_s series resistance and its intercept on the current axis gives (nkT/q). To obtain φ_B barrier height, Cheung and Cheung defined a function as

$$H(I) = V + \frac{nkT}{q} \ln\left(\frac{I}{AA^*T^2}\right) = IR_s + n\varphi_B \tag{8}$$

Similarly, the plot of $H(I)$ vs. I gives the series resistance R_s and the barrier height φ_B.

In Fig. 4, we give the plots of $(dV/d(\ln I))$ vs. I for different temperatures in a wide range from 90 to 300 K. As seen from the figure, the curves show very good linearity for all temperatures over the range considered. The values of n and R_s were calculated, yielding values of $n=1.32$ and $R_s=772\,\Omega$ for the metal/n-InAlAs diode at room temperature. It should be noted that the value of (n) obtained from the $dV/d(\ln I)$ vs. I curves is larger than that of the forward-bias $\ln I$ vs. V plot. This can be attributed to the effect of series resistance and interface states and to the voltage drop across the interfacial layer. The ideality factor increased from 1.32 to 1.93 as the measured temperature decreased from 300 to 90 K. While, the R_s values decreased from 772 to 125 Ω as the measured temperature decreased from 300 to 90 K.

Fig. 5 shows the plot of $H(I)$ vs. I of the diode measured at various temperatures ($A^* = 10.1$ A cm^{-2} K^{-2}). Using the value of the n obtained from Eq. (4), the value of the Schottky barrier height is obtained from the y-axis intercept. The value of the Schottky barrier height increased from 0.39 to 0.88 eV, and the series resistance increased from 153 to 847 Ω as the temperature increased from 90 to 300 K.

The barrier height and ideality that derived from the Cheung's model are summarized in Table 1. A barrier height of 0.88 eV with the ideality factor of 1.32 was obtained at the 300 K measurement. A value of 0.39 eV of the barrier height with the ideality factor of 1.93 was
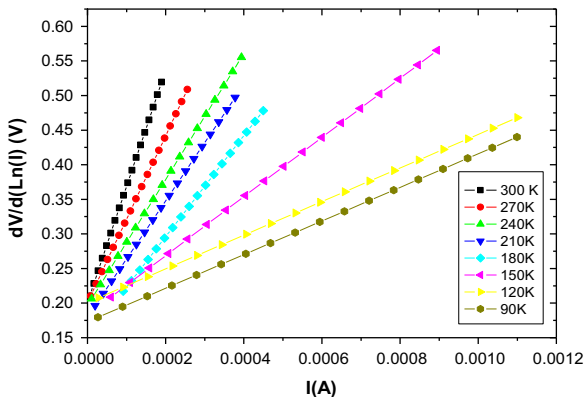

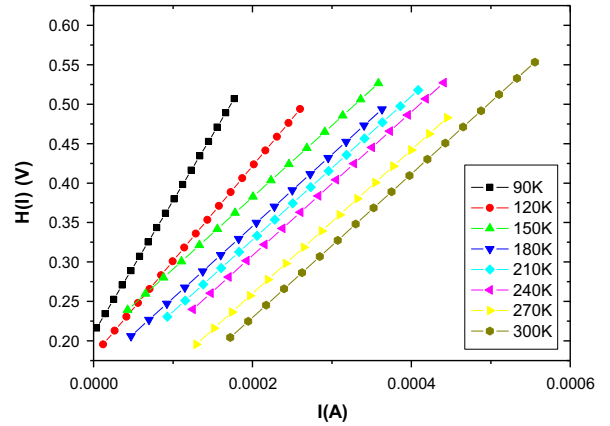**Fig.4.** Plot of $dV/d(\ln I)$ vs. I for metal/n-InAlAs Schottky diode at various temperatures.

Fig.5. Plot of $H(I)$ vs. I of the metal/n-InAlAs Schottky diode at various temperatures.

Table 1
Series resistance, ideality factor and barrier height values obtained by the Cheung's method and the Norde method for metal/n-InAlAs diode.

Temperature, T (K)	$dV/d(\ln I)$		$H(I)$		$F(V)$	
	n	R_s (Ω)	ϕ_b (eV)	R_s (Ω)	ϕ_b (eV)	R_s (Ω)
90	1.93	125	0.39	153	0.41	213
120	1.81	154	0.42	181	0.46	241
150	1.62	179	0.49	208	0.51	269
180	1.57	235	0.52	261	0.54	322
210	1.46	308	0.57	317	0.61	488
240	1.41	440	0.68	448	0.69	672
270	1.38	599	0.79	636	0.81	807
300	1.32	772	0.88	847	0.89	966

obtained at the 90 K measurement. The barrier height increased and the factor decreased as the temperature is increased. Similar results are also obtained from the TE model of the diode.

Norde proposed an alternative method to determine value of the series resistance [34]. The following function has been defined in the modified Norde's method [35]

$$F(V) = \frac{V}{2} - \frac{kT}{q} \ln\left(\frac{I(V)}{AA^*T^2}\right) \tag{9}$$

The current $I(V)$ is obtained from the I–V curves at each temperature in Fig. 1. Fig. 6 shows the $F(V)$ vs. V plots obtained using the I–V data ($A^* = 10.1$ A cm^{-2} K^{-2}). The BH relation can be given as follows:

$$\varphi_B = F(V_{min}) + \frac{V_{min}}{2} - \frac{kT}{q} \tag{10}$$

where $F(V_{min})$ is the minimum value of $F(V)$ and the corresponding voltage is V_{min}. The series resistance R_s can be expressed as

$$R_s = \frac{(2-n)kT}{qI_{min}} \tag{11}$$

where I_{min} is the value of the forward current at the voltage V_{min} where the function $F(V)$ exhibits a minimum.
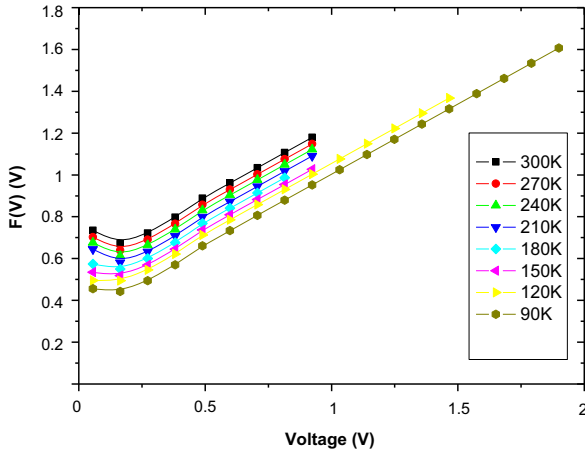
Fig.6. Plot of $F(V)$ vs. V of the metal/n-InAlAs Schottky diode at various temperatures.

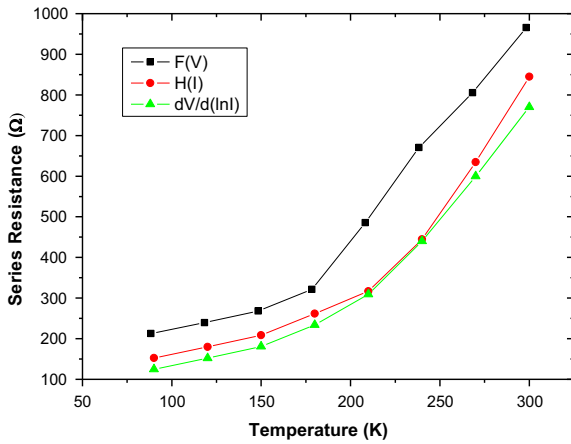**Fig. 8.** The Richardson plot of the metal/n-InAlAs.

Fig. 7. Temperature dependence of the series resistances obtained from various methods for metal/n-InAlAs.

The series resistance values from the curves as a function of temperature are given in Fig. 7. The series resistance values vary from 966 Ω at 300 K to 213 at 90 K.

The comparison of R_s obtained from the Cheung's method and Nord's function is shown in Fig. 7. There is an agreement in the value of R_s obtained from dV/d(ln$I$)–I and $H(I)$–I curves. However, the value of series resistance obtained from Norde function is higher than that obtained from Cheung function. Cheung function are only applied to the nonlinear region in high voltage section of the forward-bias ln(I)–V characteristics, while the Norde's model may not be suitable method especially for the high ideality factor of the rectifying junctions, which are non-agreed with pure thermionic emission theory. Therefore, R_s value from Norde functions can be much higher than the Cheung model for especially non-ideal rectifying structures [36]. As can be seen in Fig. 7, the series resistance increases with increasing temperature, as could be expected for semiconductors in the temperature range region where there is no carrier freezing out, which is non-
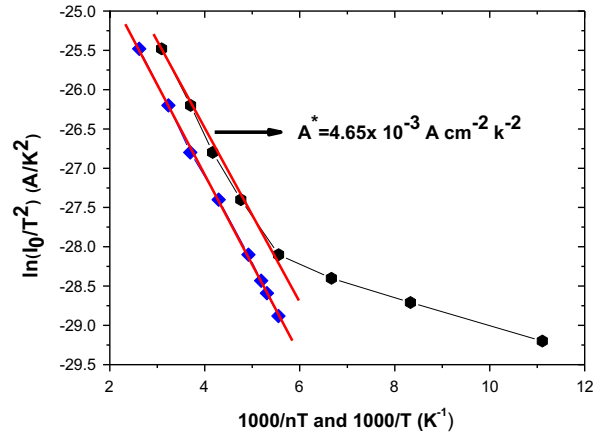
negligible below 90 K. Similar results were obtained in literature [37–38].

Fig. 8 shows the Richardson plot of $\ln(I_s/T^2)$ vs. $1000/T$ and $1000/nT$. The dependence of $\ln(I_s/T^2)$ vs. $1000/T$ is found to be non-linear in the temperature measured; however, the dependence of $\ln(I_s/T^2)$ vs. $1000/nT$ gives a straight line. The non-linearity of the conventional $\ln(I_s/T^2)$ vs. $1000/T$ is due to the temperature dependence of the barrier height and ideality factor. The Richardson constant of 4.65×10^{-3} A cm^{-2} K^{-2}, which is much lower than the known value of 10.1 A cm^{-2} K^{-2} for InAlAs was obtained. The deviation in the Richardson plots was mainly due to the spatially inhomogeneous barrier heights and potential fluctuations at the contact interface [26,39]. That is, for the passing through of the carrier to the metal/semiconductor junction, it preferentially passed through the lower barrier in the potential distribution.

The Schottky barrier height inhomogeneity of the metal/n-InAlAs diode was considered by Gaussian distribution of the barrier heights. It assumed a Gaussian distribution of the Schottky barrier heights with a mean value $\overline{\varphi}_b$ and a standard deviation σ_s. The relations are shown below [26]

$$P(\varphi_b) = \frac{1}{\sigma_s\sqrt{2\pi}} \exp\left[-(\varphi_b) - \frac{\overline{\varphi}_b}{2\sigma_s^2} \right] \quad (12)$$

where $(1/\sigma_s\sqrt{2\pi})$ is the normalization constant.

The total current I at the forward bias voltage V is given by [40]

$$I(V) = \int_{-\infty}^{+\infty} I(\varphi_b, V) P(\varphi_b) d\varphi \quad (13)$$

On integration, the total current can be expressed as [41],

$$I(V) = I_0 \exp\left(\frac{qV}{n_{ap}kT}\right) \left[1 - \exp\left(-\frac{qV}{kT} \right) \right] \quad (14)$$

where

$$I_0 = AA^*T^2 \exp\left(-\frac{q\varphi_{ap}}{kT} \right) \quad (15)$$

The parameters, I_s is saturation current, φ_{ap} is apparent barrier height and n_{ap} is apparent ideality factor at

zero bias, respectively. The apparent barrier height and apparent ideality can be expressed as [42–44]

$$\varphi_{ap} = \overline{\varphi}_{b0}(T=0) - \frac{q\sigma_{so}^2}{2kT} \qquad (16)$$

$$\left(\frac{1}{n_{ap}} - 1\right) = \rho_2 - \frac{q\rho_3}{2kT} \qquad (17)$$

It is assumed that the standard deviation σ_s and the mean value of the Schottky barrier height $\overline{\varphi}_b$ are the voltages dependent. These voltages are dependent linearly on Gaussian parameters that are given by $\overline{\varphi}_b = \overline{\varphi}_{b0} + \rho_2 V$ and $\sigma_s = \sigma_{so} + \rho_3 V$, where ρ_2 and ρ_3 are the voltage coefficients that depend on the temperature and they quantify the voltage deformation of the barrier height distribution.

Fig. 9 shows the Schottky barrier height and ideality factor vs. $1/T$ of the metal/n-InAlAs Schottky diode according to Gaussian distribution of the barrier heights. The plot of φ_{ap} vs. $1/2 kT$ gives a straight line, and $\overline{\varphi}_{b0}$ and σ_{so} are obtained from the intercept and slope, respectively. Fitting the experimental data into Eqs. (2) or (15) and in Eq. (4) gives Φ_{ap} and n_{ap}, respectively, which should obey Eqs. (16) and (17). The mean value $\overline{\varphi}_{b0}$ is 0.96 eV and standard deviation σ_{so} is equal to 0.128 V, respectively. For a homogeneous barrier height, its value of σ_{so} should be very small. On the other hand, a larger value of σ_{so} will give a inhomogeneous Schottky barrier height. The value of σ_{so} (0.128 V) is not small. It shows the existence of the inhomogeneous of barrier between at the junction of the metal–InAlAs diode. The temperature dependence of the ideality factor can be evaluated through equation $n = q/kT[\partial V / \partial(\ln I)]$. The fitting data of the ideality factor is shown in Fig. 9. The fitting data showed a straight line that gives voltage coefficients ρ_2 and ρ_3 from the intercept and slope of the plot where $\rho_2 = 0.21$ and $\rho_3 = 0.23$ V from the experimental data. The linear behavior of the $(n^{-1} - 1)$ vs. $(q/2kT)$ plot confirms that the ideality factor does indeed denote the voltage deformation of the Gaussian distribution of the barrier height.
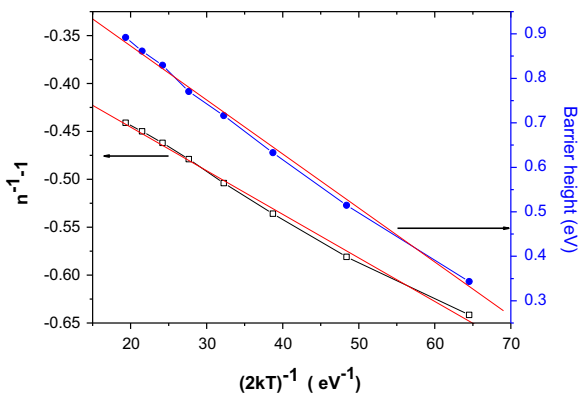

Fig. 9. The barrier height and ideality factor vs. $1/2 kT$ of the metal/n-InAlAs Schottky diode according to Gaussian distribution of the barrier heights.
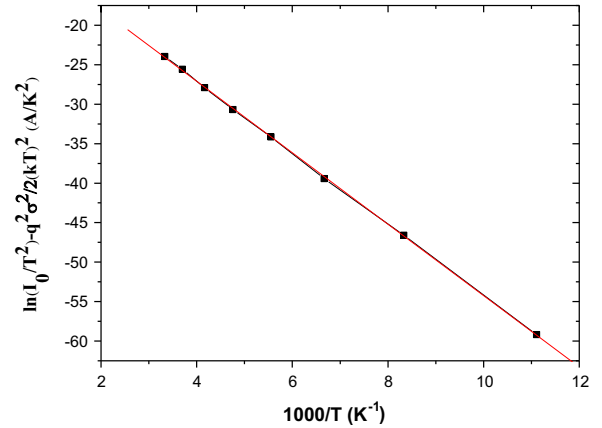

Fig. 10. The modified Richardson plot of metal/n-InAlAs diode according to Gaussian distribution of the barrier heights.

By combining Eqs. (15) and (16), a relation of modified Richardson plot can be obtained. The equation is shown as

$$\ln\left(\frac{I_0}{T^2}\right) - \left(\frac{q 2\sigma_{so}^2}{2k^2 T^2}\right) = \ln(AA^*) - q\frac{\overline{\varphi}_{b0}}{kT} \qquad (18)$$

The modified Richardson plot $\ln(I_0/T^2) - (q^2\sigma_{so}^2/2k^2T^2)$ vs. $1000/T$ of the diodes was obtained and shown in Fig. 10. The plot according to Eq. (18) should also be a straight line with the slope and the intercept at the ordinate directly yielding the mean barrier height $\overline{\varphi}_{b0}$ and A^*, respectively. It can be seen that the modified Richardson plot has a quite good linearity over the whole temperature range. It corresponds to activation energy around $\overline{\varphi}_{b0}$. By fitting of the data, $\overline{\varphi}_{b0} = 0.98$ eV and $A^* = 9.2$ A cm^{-2} K^{-2} are obtained. The value of activation energy (0.98 eV) is very close to the mean value barrier height (0.96 eV). The Richardson constants are in close agreement with the theoretical value of A^* which is 10.1 A cm^{-2} K^{-2}. For an unmodified Richardson plots, it shows the activation energy of 0.47 eV and the Richardson constant is equal to 4.65×10^{-3} A cm^{-2} K^{-2}. The deviation in the Richardson plots proved the spatially inhomogeneous barrier heights and potential fluctuations at the junction interface. While, as the inhomogeneous effects by Gauss distribution was taken into consideration, the modified Richardson plot shows a straight line relationship between $\ln(I_0/T^2) - (q^2\sigma_{so}^2/2k^2T^2)$ vs. $1000/T$, and gives reasonable value of Richardson constant.

4. Conclusion

In conclusion, the $I-V-T$ characteristics of metal/InAlAs Schottky contact on n-type InP have been measured in the temperature range 90–300 K. It shows an abnormal increase of the barrier height and decrease of ideality factor as the measure temperature is increased. Similar phenomena are also found by the Cheung and Cheung's model. The series resistance is evaluated and it is found that the series resistance increased as the increase of the measured temperature. The distribution of the barrier height is inhomogeneous that is present at the interface. These characteristics have been interpreted on the basis of

the TE mechanism with Gaussian distribution of the barrier heights of $\overline{\varphi}_{b0}$ which is 0.96 eV and standard deviation σ_{so} which is equal to 0.128 V. In addition, the Richardson plot and modified Richardson give the evidence of the spatial inhomogeneous barrier heights and potential fluctuations at the interface.

References

[1] W. Monch, Semiconductor Surfaces and Interfaces, 3rd ed. Springer, Berlin, 2001.
[2] H. von Wenckstern, G. Biehne, R.A. Rahman, H. Hochmuth, M. Lorenz, M. Grundmann, Appl. Phys. Lett. 88 (2006) 092102.
[3] K. Ahmed, T. Chiang, Appl. Phys. Lett. 102 (2013) 042110.
[4] S. Demirezen, Ş. Altındal, Curr. Appl. Phys. 10 (2010) 1188.
[5] H. Tecimer, A. Türüt, H. Uslu, Ş. Altındal, İ. Uslu, Sens. Actuators A: Phys. 199 (2013) 194.
[6] E. Özavcı, S. Demirezen, U. Aydemir, Ş. Altındal, Sens. Actuators A: Phys. 194 (2013) 259.
[7] R.T. Tung, Phys. Rev. B 45 (1992) 13509.
[8] F.A. Padovani, in: in: R.K. Willardson, A.C. Beer (Eds.), Semiconductors and Semimetals, vol. 7A, Academic Press, New York, 1971.
[9] C.R. Crowell, Solid State Electron. 20 (1977) 171.
[10] R.T. Tung, J.P. Sullivan, F. Schrey, Mater. Sci. Eng. B 14 (1992) 266.
[11] R.F. Schmitsdrof, T.U. Kampen, W. Mnch, J. Vac. Sci. Technol. B 15 (1997) 1221.
[12] S.Y. Zhu, R.L. Van Meirhaeghe, C. Detavernier, F. Cordan, G.P. Ru, X.P. Qu, B.Z. Li, Solid State Electron. 44 (2000) 663.
[13] H.J. Im, Y. Ding, J.P. Pelz, W.J. Choyke, Phys. Rev. B 64 (7) (2001) 075310.
[14] R.C. Rossi, M.X. Tan, N.S. Lewis., Appl. Phys. Lett. 77 (17) (2000) 2698.
[15] R.C. Rossi, N.S. Lewis, J. Phys. Chem. B 105 (17) (2001) 12303.
[16] W.C. Hsu, D.H. Huang, Y.S. Lin, Y.J. Chen, J.C. Huang, C.L. Wu, IEEE Trans. Electron. Dev. 53 (2006) 406.
[17] J.H. Tsai, C.M. Li, Solid-State Electron. 52 (2008) 146.
[18] N. Hamdaoui, R. Ajjel, H. Maaref, B. Salem, G. Bremond, M. Gendry., Semicond. Sci. Technol. 25 (2010) 065011.
[19] N. Hamdaoui, R. Ajjel, B. Salem, M. Gendry, H. Maaref., Physica B 406 (2011) 3531.
[20] J.A. Silberman, T.J. de Lyon, J.M. Woodall, Appl. Phys. Lett. 58 (1991) 2126.
[21] H.K. Henisch, Semiconductor ContactsLondon, Oxford University123.
[22] C.W. Wilmsen, Physics and Chemistry of III–V Compound Semiconductor Interfaces, Plenum, New York, 1985.
[23] E.D. Palic, R.F. Wallis, Phys. Rev. 123 (1961) 131.
[24] D.J. Stukel, R.N. Euwema, Phys. Rev. 188 (1969) 1193.
[25] Landolt-Bornstein, Springer, Berlin, 1982, vol. 17a.
[26] J.H. Werner, H.H. Guttler, J. Appl. Phys. 69 (1991) 1522.
[27] S. Shankar Naik, V. Rajagopal Reddy., Superlattices Microstruct. 48 (2010) 330.
[28] M.E. Aydin, et al., Physica B 387 (2007) 239.
[29] O. Gullu, A. Turut, Microelectron. Eng. 87 (2010) 2482.
[30] F.A. Padovani, G. Sumner, J. Appl. Phys. 36 (1965) 3744.
[31] Z. Horvath, Solid State Electron. 36 (1996) 176.
[32] S.K. Tripathi, J. Mater. Sci. 45 (2010) 5468.
[33] S.K. Cheung, N.W. Cheung, Appl. Phys. Lett. 49 (1986) 85.
[34] H. Nordde, J. Appl. Phys. 50 (1979) 5052.
[35] S. Karatas, S. Altindal, A. Turut, M. Cakar, Physica B 392 (2007) 43.
[36] S. Aydogan, M. Saglam, A. Turut, Y. Onganer, Mater. Sci. Eng. C 29 (2009) 1486.
[37] I. Dokme, Ş. Altındal, Semicond. Sci. Technol. 21 (2006) 1053.
[38] K.H. Baik, Y. Irokawa, F. Ren, S.J. Pearton, S.S. Park, Y.J. Park, Solid-State Electron. 47 (2003) 1533.
[39] H.H. Guttler, J.H. Werner, Appl. Phys. Lett. 56 (1990) 1113.
[40] S. Chand, J. Kumar, J. Appl. Phys. 80 (1) (1996) 288.
[41] Y.P. Song, R.L. Van Meirhaeghe, W.H. Laflere, F. Cardon, Solid-State Electron. 29 (1986) 633.
[42] M.K. Hudait, K.P. Venkateswarlu, S.B. Krupanidhi, Solid State Electron. 45 (2001) 133.
[43] S. Zhu, R.L. Van Meirhaeghe, C. Detavernier, F. Cardon, G.P. Ru, X.P. Qu, et al., Solid-State Electron. 44 (2000) 663.
[44] Y.P. Song, R.L. Van Meirhaeghe, W.H. Laflere, F. Cardon, Solid-State Electron. 29 (1986) 663.